Heisenberg treatment of pair generation in lossy coupled-cavity systems

M. Kamandar Dezfouli* and M. M. Dignam
Department of Physics, Engineering Physics and Astronomy, Queen's University, Kingston, Ontario K7L 3N6, Canada

M. J. Steel
Centre for Ultrahigh bandwidth Devices for Optical Systems (CUDOS), MQ Photonics Research Centre, Department of Physics and Astronomy, Macquarie University, Sydney, NSW 2109, Australia

J. E. Sipe
Department of Physics and Institute for Optical Sciences, University of Toronto, 60 St. George Street, Toronto, Ontario M5S 1A7, Canada
(Received 26 June 2014; published 17 October 2014)

We employ a quasimode representation of the adjoint master equation to study nonlinear pair-generation dynamics via spontaneous four-wave mixing in coupled-cavity systems in the presence of scattering loss. Perturbative analytic solutions for signal and idler photon-number operators are derived, which enable us to examine the effect of scattering loss on pair-generation dynamics. In particular, for a simple three-mode system, we show that any loss mismatch for the signal and idler photons increases the probability of finding unpaired photons. While decreasing the loss rates for signal and idler photons increases the pair signal brightness, it also results in higher generation rates for multiple pairs in the system, which can result in lower operational signal-to-noise ratios.

DOI: 10.1103/PhysRevA.90.043832 PACS number(s): 42.65.Lm, 42.50.Ct, 42.60.Da

I. INTRODUCTION

Photon pair generation through nonlinear processes is of great importance in quantum photonic applications, particularly as a means to obtain heralded single-photon sources for on-chip integrated devices. This is true for systems both with cubic [1–35] and with quadratic [36–47] nonlinearities. Due to the generally low material nonlinearity, high pump intensities over the nonlinear region are needed to achieve a bright signal. Optical microring resonators [3,4,30,48–51], photonic crystal waveguides [5,35], and photonic molecules in photonic crystal slabs [52–55] have been used to enhance the nonlinear interaction by exploiting the strong light confinement. In addition, exploiting slow light in coupled-resonator optical waveguides (CROWs) [7,32,33,56,57] has been proposed to achieve a high light intensity in the nonlinear region. However, the confined optical modes in both ring resonators and point defects in photonic crystal slabs have finite lifetimes due to the leakage of light out of the system. This is associated with both the intrinsic leakiness of the localized optical resonances and the scattering loss due to fabrication imperfections. This has implications for device design, as one has to balance scattering loss, dispersion, and generation in optimizing the system parameters. For convenience, we refer to both types of dissipation as "scattering loss" or "leakage" and distinguish this loss from material absorption, which we do not consider here. Photon loss can also result in false heralding. For example, in a heralded single-photon source, the signal photon might not be delivered to the output port of the device even when the heralding idler detector has already clicked. It is therefore necessary to understand the role scattering loss plays during the generation process.

In addition to loss, multiple pair generation [58] is a key consideration in the design of a heralded single-photon source. Multiple pair generation can result in more than one signal photon being delivered to a quantum circuit or apparatus, even when the heralding detector fires only once. Since typically only one photon per qubit mode should be delivered to the next unit on an integrated chip, the presence of multiple photons due to higher order pair generation would likely result in faulty operation. Although dark counts contribute to noise for a low pump power, when the pump power is high the effect of higher order pair generation is usually the main contributor to the observed signal-to-noise ratio, commonly described in the experimental literature as the "coincidence-to-accidental ratio" (CAR). Therefore, it is important to examine the effect of leakage loss on multiple pair generation in coupled-cavity systems.

There is of course an enormous literature on the theoretical treatment of classical and quantum nonlinear optical processes in microcavities, waveguides, and coupled-cavity waveguide systems [59–64]. Here we consider the cubic nonlinear process of spontaneous four-wave mixing (SFWM), where, as usual, we imagine pumping the system in one frequency range and looking for signal and idler photons in neighboring frequency bands (see Fig. 1). SFWM is a central area of study in contemporary quantum photonics because of its potential for providing an on-demand photon source [65], and it is increasingly being studied experimentally in nanophotonic and resonant structures [66–71]. Yet the effects of loss in a quantum mechanical picture have been treated only in optical fibers, silicon waveguides, and silicon wire waveguides [67,68,70,71]. To the best of our knowledge, a fully quantum mechanical treatment of effects of scattering loss during the SFWM pair-generation process in photonic coupled-cavity systems has not been presented to date.

In this paper, we present a theoretical model of SFWM in lossy coupled-cavity structures. Our aim is to address the

*m.kamandar@physics.queensu.ca

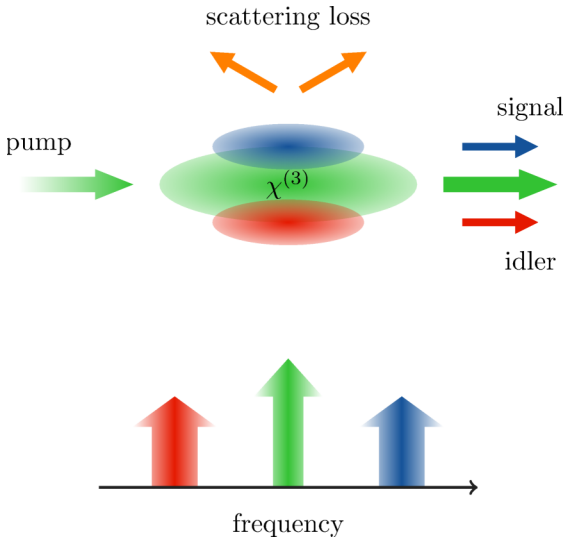

FIG. 1. (Color online) Schematic of four-wave mixing process. Two pump photons convert into signal and idler photons. Top: Spatial extent of the three pump, signal, and idler modes is shown. They all need to overlap over the nonlinear region of the system. Bottom: Energy conservation, $\omega_s + \omega_i = 2\omega_p$, selects the generated pair frequencies for a given pump frequency. The diagram shows excitation over a range of frequencies which turns into pair generation over neighboring ranges of frequencies.

leakage loss in these structures and the way it affects the pair-generation process. Indeed, we develop a general formalism to treat nonlinear quantum interactions with scattering loss. Our approach is quite general and could be applied to any system for which a mode basis can be defined, such as coupled photonic crystal cavities or microring resonators coupled to straight waveguides. The formalism could also be applied to a variety of other nonlinear processes, including, most obviously, spontaneous parametric down conversion.

The basis of the method is to formulate the pair generation in leaky coupled-cavity systems in terms of a "quasimode" (QM) basis [72]. QMs are the leaky modes of the system with complex frequencies, the imaginary part of which describes the photon loss into regions beyond the system of interest. By using QMs, the intrinsic loss in these systems is naturally included in the formalism. Following previous work by two of us [73], which established a general QM formalism for nonlinear quantum optics, we first project the full Hamiltonian of the system onto the QM basis. We then use the QM representation of the adjoint quantum master equation [73,74] to calculate the time evolution for different operators. Alternatively, one could solve the quantum master equation itself to obtain the time evolution for the photon density matrix. However, as we show, solving the less familiar adjoint master equation for Heisenberg operators simplifies the calculations.

The paper is organized as follows. In Sec. II, the QM formulation of nonlinear pair generation is presented. In Sec. III, the Heisenberg time evolution of various photon-number operators is derived. In Sec. IV, the lossy photon dynamics for the signal and idler is discussed for a simple model that has only three modes resonant with the signal, idler, and pump frequencies. In Sec. V, the effects of multiple pair generation and loss on multiple pair generation is presented for the same model. Finally, in Sec. VI, we present our conclusions.

II. QUASIMODE REPRESENTATION OF THE ADJOINT MASTER EQUATION

To envisage a process of pair generation through the $\chi^{(3)}$ nonlinearity in a coupled resonator system, such as a CROW or a "photonic molecule," we begin by setting up the QM representation. A full discussion and derivation of key results can be found in earlier work [73].

We denote the spatial profile of a QM by the complex electric field $\tilde{\mathbf{N}}_m(\mathbf{r})$, so that the complete classical electric field is given by

$$\mathbf{E}(\mathbf{r},t) = \sum_m [\tilde{c}_m \tilde{\mathbf{N}}_m(\mathbf{r}) e^{-i\tilde{\omega}_m t} + \text{c.c.}], \tag{1}$$

where the $\tilde{c}_m$ are expansion coefficients and c.c. is the complex conjugate. The mode is associated with a complex frequency, $\tilde{\omega}_m = \omega_m - i\gamma_m$, the imaginary part of which, γ_m, is the field loss rate due to scattering loss. Throughout, we use a tilde to differentiate complex modes and frequencies from real-valued ones. QMs are the solutions to Maxwell's equations and can be found numerically using, for example, the finite-difference time-domain method for individual defects with outgoing boundary conditions or by seeking the poles in frequency-domain solvers. The QM is extended over all space, but most of the field density is confined within a finite volume that contains the defects (cavities) of interest as well as some of the surrounding space. Therefore, a computational volume, V_c, is chosen such that the calculated mode within gives accurate information, as long as near-field considerations are concerned. If needed, for complicated structures made of several defects, the tight-binding approach may be employed to obtain the QMs of the coupled-cavity system [72] based on the modes of the individual cavities calculated numerically.

In general, QMs overlap in both frequency and space, so they form a nonorthogonal basis; while workable [73], this does bring some complexity to a typical quantum optical calculation of photon dynamics. However, for the purpose of this work, we assume the existence of an orthogonal QM basis, which could be a consequence of the underlying symmetry of the structure of interest. For example, an infinitely long CROW structure can be described by an orthogonal continuous infinite basis of modes. Although, the generalization to a continuum is straightforward, for simplicity we choose to work with a discrete basis, the elements of which we label with index n.

A. The linear Hamiltonian

We begin with the projection of the linear part of the electromagnetic Hamiltonian onto the QM basis. Using the Einstein summation convention, the linear Hamiltonian operator can be shown to be [75]

$$H_{\mathrm{L}} = \frac{\epsilon_o}{2} \int d^3\mathbf{r}\, \epsilon(\mathbf{r})\, E_i(\mathbf{r},t)\, E_i(\mathbf{r},t) + \frac{1}{2\mu_o} \int d^3\mathbf{r} B_i(\mathbf{r},t)\, B_i(\mathbf{r},t), \tag{2}$$

where i labels the component of the field, $\epsilon(\mathbf{r})$ is the relative dielectric constant, and E_i and B_i are the components of the electric and magnetic field operators. We have assumed an isotropic response for the material and have neglected the material dispersion. Using an expansion in true modes, the usual electric field operator in the absence of a nonlinear interaction is

$$E_i(\mathbf{r},t) = \int d\mu \sqrt{\frac{\hbar\omega_\mu}{2\epsilon_0}} f_{\mu i}(\mathbf{r})\, e^{-i\omega_\mu t} a_\mu + \text{H.c.}, \tag{3}$$

where $f_{\mu i}(\mathbf{r})$ are standard functions inside a large quantization volume and H.c. denotes the Hermitian conjugate. To simplify the notation, we take μ to be a set of four indices identifying the spatial and polarization properties of the mode. The usual quantized Hamiltonian of the linear part is then

$$H_\text{L} = \int d\mu\, \hbar\omega_\mu a_\mu^\dagger a_\mu, \tag{4}$$

where ω_μ is the mode frequency and the vacuum energy has been dropped. The a_μ and $a_\mu^\dagger$ are the ladder operators of the μth true mode, which, in the continuum limit, satisfy the normal bosonic commutation relation $[a_\mu, a_{\mu'}^\dagger] = \delta(\mu - \mu')$, where $\delta(\mu)$ is a generalized δ function including a discrete Kronecker δ function for polarization and a continuous Dirac δ function for the spatial part of the mode index, when the size of the box is allowed to go to infinity. These are time-independent Schrödinger operators, as opposed to the time-dependent Heisenberg operators that we use later to carry out photon dynamics calculations. Unless the time dependence is explicitly indicated, the raising and lowering operators are taken to be Schrödinger operators. We note that frequencies involved in this standard representation are real quantities, in contrast to our QM approach, where we deal with modes with complex frequencies.

The philosophy of the QM approach is to address scattering loss in a natural manner. As the detailed derivation of our QM approach is rather involved and is presented elsewhere [73], in this work we only outline the general procedure and key results. Using the fact that the QMs can, in principle, be expanded in the basis of true modes, we define a non-Hermitian quantum projector operator to project the system Hamiltonian from the basis of the true modes onto the basis of the QMs. Following [73], the projected linear Hamiltonian in the QM basis is given by

$$\tilde{H}_\text{L} = \sum_m \hbar\tilde{\omega}_m b_m^\dagger b_m, \tag{5}$$

where the corresponding ladder operators for different QMs satisfy the normal bosonic commutation relation, $[b_m, b_n^\dagger] = \delta_{mn}$. Note that the projected linear Hamiltonian is now non-Hermitian. This simply indicates energy loss from the volume of the interest via different QMs.

As shown earlier [73], the projected Hamiltonian can then be used to construct the master equation by using the Heisenberg equations of motion in the QM basis and then including the proper norm-conserving terms for the density matrix. From this, the corresponding adjoint master equation for a given Heisenberg operator, $\hat{A}(t)$, can be derived as [73]

$$\frac{d\hat{A}_H(t)}{dt} = -\frac{i}{\hbar}\left(\hat{A}_H(t)\tilde{H}_\text{L} - \tilde{H}_\text{L}^\dagger \hat{A}_H(t)\right) + 2\sum_m \gamma_m b_m^\dagger \hat{A}_H(t) b_m. \tag{6}$$

This is similar to the normal Heisenberg equation except for the fact that the Hamiltonian in non-Hermitian and the extra norm-conserving terms are present. If we introduce the Hermitian operator

$$H_\text{L} = \sum_m \hbar\omega_m b_m^\dagger b_m \tag{7}$$

and the dissipation rate $\Gamma_m = 2\gamma_m$, then Eq. (6) is equivalent to the usual master equation of Lindblad form [74]:

$$\frac{d\hat{A}_H(t)}{dt} = -\frac{i}{\hbar}[\hat{A}_H(t), H_\text{L}] + \sum_m \Gamma_m \left(b_m \hat{A}_H(t) b_m^\dagger - \frac{1}{2}\hat{A}_H(t) b_m^\dagger b_m - \frac{1}{2} b_m^\dagger b_m \hat{A}_H(t) \right). \tag{8}$$

To see the practical advantage of working in the QM basis, we rewrite Eq. (6) in the following form:

$$\frac{d\hat{A}_H(t)}{dt} = \mathcal{L}_0(\hat{A}_H(t)) \tag{9}$$

$$\equiv \frac{i}{\hbar}\sum_m \hbar\tilde{\omega}_m [b_m^\dagger, \hat{A}_H(t)] b_m + \frac{i}{\hbar}\sum_m \hbar\tilde{\omega}_m^* b_m^\dagger [b_m, \hat{A}_H(t)]. \tag{10}$$

This equation yields simple Heisenberg dynamics for any normally ordered product of ladder operators under the time evolution of the linear Hamiltonian of the system. As an example, in the simple case of the destruction operator, we have

$$\frac{db_n(t)}{dt} = \frac{i}{\hbar}\sum_m \hbar\tilde{\omega}_m [b_m^\dagger, b_n(t)] b_m + \frac{i}{\hbar}\sum_m \hbar\tilde{\omega}_m^* b_m^\dagger [b_m, b_n(t)], \tag{11}$$

where we emphasize that the operators without explicit time dependence are Schrödinger operators.

Using the ansatz $b_n(t) \equiv f_n(t) b_n$, it is easy to see that

$$\frac{db_n(t)}{dt} = -i\tilde{\omega}_n b_n(t), \tag{12}$$

and similarly,

$$\frac{db_n^\dagger(t)}{dt} = i\tilde{\omega}_n^* b_n^\dagger(t), \tag{13}$$

as expected. It is also easy to see that

$$\frac{d(b_{n_1}^\dagger b_{n_2})(t)}{dt} = i(\tilde{\omega}_{n_1}^* - \tilde{\omega}_{n_2})(b_{n_1}^\dagger b_{n_2})(t). \tag{14}$$

The parentheses around the two operators indicate that this pair of operators is to be considered one Heisenberg operator. We

use this notation because, in the presence of the nonlinearity, in general for an operator $\hat{C} \equiv \hat{A}\hat{B}$, $\hat{C}(t) \equiv (\hat{A}\hat{B})(t) \neq \hat{A}(t)\hat{B}(t)$. When there is no nonlinearity present, then for some operator combinations, $(\hat{A}\hat{B})(t) = \hat{A}(t)\hat{B}(t)$. For example, we see from Eq. (14) that the number operator $(b_n^\dagger b_n)(t)$ decays exponentially as expected from the evolution of $b_n^\dagger(t)$ and $b_n(t)$. When there is no nonlinearity, this can be generalized to any normally ordered combination of ladder operators, e.g.,

$$\frac{d(b_{n_1}^\dagger b_{n_2}^\dagger b_{n_3}^\dagger b_{n_4} b_{n_5})(t)}{dt} = i\left(\tilde{\omega}_{n_1}^* + \tilde{\omega}_{n_2}^* + \tilde{\omega}_{n_3}^* - \tilde{\omega}_{n_4} - \tilde{\omega}_{n_5}\right) \times (b_{n_1}^\dagger b_{n_2}^\dagger b_{n_3}^\dagger b_{n_4} b_{n_5})(t). \quad (15)$$

This is quite powerful, because any operator can be written as sums of products of normally ordered ladder operators.

B. Nonlinear Hamiltonian treatment

In this section, we add the nonlinear part of the Hamiltonian corresponding to four-wave mixing interactions to the model. The full form of the adjoint master equation becomes

$$\frac{d\hat{A}_H(t)}{dt} = \mathcal{L}_0(\hat{A}_H(t)) - \frac{i}{\hbar}[\hat{A}_H(t), \tilde{H}_{\rm NL}], \quad (16)$$

where $\tilde{H}_{\rm NL}$ is the projected Hermitian nonlinear Hamiltonian in the QM basis. Here, for simplicity of notation we retain the tilde (even though the nonlinear Hamiltonian is Hermitian) to represent the nonlinear Hamiltonian projected on the basis of the QMs.

Following [75], the nonlinear part of the Hamiltonian responsible for the SFWM process in the standard representation is

$$H_{\rm NL} = -\frac{1}{4\epsilon_o}\int d^3\mathbf{r}\, \Gamma^{(3)}_{ijkl}(\mathbf{r}) \times D_i(\mathbf{r},t)\, D_j(\mathbf{r},t)\, D_k(\mathbf{r},t)\, D_l(\mathbf{r},t), \quad (17)$$

where $\mathbf{D}$ is the electric displacement and $\Gamma^{(3)}$ is the nonlinear response tensor appropriate for the expansion in $\mathbf{D}$, which is related to the standard third-order susceptibility tensor, $\chi^{(3)}_{ijkl}$ [63]. Employing QM projection techniques [73], it can be shown that the QM representation of this nonlinear Hamiltonian is

$$\tilde{H}_{\rm NL} = -\sum_{m_1,m_2}\sum_{p_1,p_2} \hbar\, S_{m_1,m_2,p_1,p_2}\, b_{m_1}^\dagger b_{m_2}^\dagger b_{p_1} b_{p_2} + \text{H.c.},$$

where

$$S_{m_1,m_2,p_1,p_2} \equiv \frac{\hbar\epsilon_o}{16}\sqrt{\omega_{m_1}\omega_{m_2}\omega_{p_1}\omega_{p_2}}\int d^3\mathbf{r}\, \Gamma^{(3)}_{ijkl}(\mathbf{r})\epsilon^4 \times (\mathbf{r})\tilde{N}^*_{m_1,i}(\mathbf{r})\tilde{N}^*_{m_2,j}(\mathbf{r})\tilde{N}_{p_1,k}(\mathbf{r})\tilde{N}_{p_2,l}(\mathbf{r}). \quad (18)$$

Here, m_1 and m_2 label signal and idler modes in the SFWM process, while p_1 and p_2 label the pump modes. The subscripts, i, j, k, and l label the components of the fields and nonlinear tensor. In deriving Eq. (18), we have assumed that the imaginary parts of the complex QM frequencies are small. The quantity S represents the strength of the effective nonlinear interaction between different QMs and is negligible unless the QMs overlap significantly in the nonlinear region. As the $\chi^{(3)}$ nonlinearity is weak, S_{m_1,m_2,p_1,p_2} provides a natural expansion parameter for the perturbation treatment to follow.

In general, analytic solutions to the adjoint master equation, (16), are not available. However, as shown in the next section, analytic expressions for the time evolution of the operators of interest can be obtained using perturbation theory applied to the nonlinear Hamiltonian.

III. HEISENBERG EVOLUTION OF NUMBER OPERATORS

Signal and idler photon statistics are of primary interest in a typical pair-generation experiment. In order to detect the signal and idler photons unambiguously, we assume that their frequencies are well separated from the pump frequency and from each other [76]. Thus, the goal in this section is to calculate the Heisenberg time evolution for the photon-number operator as a perturbation expansion in S_{m_1,m_2,p_1,p_2} of the form

$$(b_n^\dagger b_n)(t) = (b_n^\dagger b_n)^{(0)}(t) + (b_n^\dagger b_n)^{(1)}(t) + (b_n^\dagger b_n)^{(2)}(t) + \cdots, \quad (19)$$

when the real part of the signal mode frequency ω_n is far from the pump mode band. We also calculate corresponding expressions for the photon-number products $\langle b_m^\dagger b_m b_n^\dagger b_n\rangle$.

From Eq. (16), the adjoint master equation for the photon-number operator is

$$\frac{d(b_n^\dagger b_n)(t)}{dt} = \mathcal{L}_0(b_n^\dagger b_n)(t) - \frac{i}{\hbar}[(b_n^\dagger b_n)(t), \tilde{H}_{\rm NL}]. \quad (20)$$

In the zeroth-order approximation in the nonlinear Hamiltonian, the evolution is simply

$$\frac{d(b_n^\dagger b_n)^{(0)}(t)}{dt} = \mathcal{L}_0(b_n^\dagger b_n)^{(0)}(t), \quad (21)$$

which has the elementary solution

$$(b_n^\dagger b_n)^{(0)}(t) = b_n^\dagger b_n e^{-2\gamma_n t}. \quad (22)$$

Thus photons in the signal and idler QMs decay exponentially at a rate $2\gamma_n$. Assuming that the pump field is in a lossy multimode coherent state

$$|\Phi_{\rm pump}\rangle = \prod_p e^{\alpha\phi_p b_p^\dagger - \alpha^*\phi_p^* b_p}|{\rm vac}\rangle, \quad (23)$$

then for any mode p with a frequency within the pump band we have

$$b_p|\Phi_{\rm pump}\rangle = \alpha\phi_p|\Phi_{\rm pump}\rangle, \quad (24)$$

where α is the overall coherent-state amplitude, ϕ_p is the pump amplitude for the pth mode, and $\sum_p |\phi_p|^2 = 1$. That is, the state of the pump field can be considered as a product of coherent states in different modes with amplitudes $\alpha\phi_p$. One would usually take the pump field to be nonzero only for a few QMs that are close to each other in frequency. As the signal and idler modes are in vacuum initially, the total initial state of the system factors as

$$|\Phi_i\rangle \equiv |\Phi_{\rm pump}\rangle \otimes |{\rm vac}\rangle_{si}. \quad (25)$$

where $|{\rm vac}\rangle_{si}$ is the vacuum state for the signal and idler modes. Therefore, the zeroth-order solution in Eq. (22) makes no contribution to the expectation value of the photon-number operator:

$$\langle (b_n^\dagger b_n)^{(0)}(t)\rangle = e^{-2\gamma_n t}\langle {\rm vac}|b_n^\dagger b_n|{\rm vac}\rangle = 0. \quad (26)$$

The nonlinear Hamiltonian appears in the first-order expression

$$\frac{d(b_n^\dagger b_n)^{(1)}(t)}{dt} = \mathcal{L}_0(b_n^\dagger b_n)^{(1)}(t) - \frac{i}{\hbar}[(b_n^\dagger b_n)^{(0)}(t), \tilde{H}_{\rm NL}]. \tag{27}$$

Working out the commutation relation using Eq. (22) results in

$$\frac{d(b_n^\dagger b_n)^{(1)}(t)}{dt} = \mathcal{L}_0(b_n^\dagger b_n)^{(1)}(t) + \left\{ 2ie^{-2\gamma_n t} \sum_{m_2} \sum_{p_1,p_2} S_{n,m_2,p_1,p_2} b_n^\dagger b_{m_2}^\dagger b_{p_1} b_{p_2} + \text{H.c.} \right\}. \tag{28}$$

Here we have exploited the fact that $n \neq p_1, p_2$ (since p_1 and p_2 correspond to pump modes) along with the even symmetry of S_{m_1,m_2,p_1,p_2} under m_1 and m_2 permutation. To solve Eq. (28), we try the ansatz

$$(b_n^\dagger b_n)^{(1)}(t) = \sum_{m_2} \sum_{p_1,p_2} h^{(1)}_{n,m_2,p_1,p_2}(t)\, b_n^\dagger b_{m_2}^\dagger b_{p_1} b_{p_2} + \text{H.c.}, \tag{29}$$

where $h^{(1)}_{n,m_2,p_1,p_2}(t)$ is a c-number function as the solution to our first-order dynamical equation. With this choice, the action of the signal and idler operators on the vacuum guarantees that the first-order expectation value for the number operator is 0:

$$\langle b_n^\dagger b_n \rangle^{(1)}(t) = 0. \tag{30}$$

However, we do need the first-order solution, (29), for use in the second-order approximation.

Inserting (29) into (28), and using the result for the time dependence of normally ordered (unperturbed) operators obtained from Eq. (10), we find

$$\frac{dh^{(1)}_{n,m_2,p_1,p_2}(t)}{dt} = i\left(\tilde{\omega}_n^* + \tilde{\omega}_{m_2}^* - \tilde{\omega}_{p_1} - \tilde{\omega}_{p_2}\right) h^{(1)}_{n,m_2,p_1,p_2}(t) + 2ie^{-2\gamma_n t} S_{n,m_2,p_1,p_2}. \tag{31}$$

The fact that we have obtained an ordinary differential equation for $h^{(1)}_{n,m_2,p_1,p_2}(t)$ indicates that the ansatz provides a solution. Integrating this leads to

$$h^{(1)}_{n,m_2,p_1,p_2}(t) = 2i\, S_{n,m_2,p_1,p_2} e^{i(\tilde{\omega}_n^* + \tilde{\omega}_{m_2}^* - \tilde{\omega}_{p_1} - \tilde{\omega}_{p_2})t} \times \int_0^t dt' e^{-2\gamma_n t'} e^{-i(\tilde{\omega}_n^* + \tilde{\omega}_{m_2}^* - \tilde{\omega}_{p_1} - \tilde{\omega}_{p_2})t'}. \tag{32}$$

Following a similar procedure (see Appendix A) we find that at second order, the photon-number expectation is nonzero:

$$\langle (b_n^\dagger b_n)^{(2)}(t) \rangle = 8|\alpha|^4 \,\text{Re}\left\{ \sum_{m_2} \sum_{p_1,p_2} \sum_{p_1',p_2'} S_{n,m_2,p_1,p_2} S^*_{n,m_2,p_1',p_2'} \phi_{p_1} \phi_{p_2} \phi^*_{p_1'} \phi^*_{p_2'} \times e^{i(\tilde{\omega}^*_{p_1'} + \tilde{\omega}^*_{p_2'} - \tilde{\omega}_{p_1} - \tilde{\omega}_{p_2})t} \int_0^t dt' e^{i(\tilde{\omega}_n^* + \tilde{\omega}^*_{m_2} - \tilde{\omega}^*_{p_1'} - \tilde{\omega}^*_{p_2'})t'} \int_0^{t'} dt'' e^{-i(\tilde{\omega}_n + \tilde{\omega}^*_{m_2} - \tilde{\omega}_{p_1} - \tilde{\omega}_{p_2})t''} \right\}. \tag{33}$$

Similarly (see Appendix B), the first nonzero contribution for the product of two photon-number operators is also second order in the perturbation and is given by

$$\langle (b_{n_1}^\dagger b_{n_1} b_{n_2}^\dagger b_{n_2})^{(2)}(t) \rangle = 8\,|\alpha|^4 \text{Re}\left\{ \sum_{p_1,p_2} \sum_{p_1',p_2'} S_{n_1,n_2,p_1,p_2} S^*_{n_1,n_2,p_1',p_2'} \phi_{p_1} \phi_{p_2} \phi^*_{p_1'} \phi^*_{p_2'} \times e^{i(\tilde{\omega}^*_{p_1'} + \tilde{\omega}^*_{p_2'} - \tilde{\omega}_{p_1} - \tilde{\omega}_{p_2})t} \int_0^t dt' e^{i(\tilde{\omega}^*_{n_1} + \tilde{\omega}^*_{n_2} - \tilde{\omega}^*_{p_1'} - \tilde{\omega}^*_{p_2'})t'} \int_0^{t'} dt'' e^{-i(\tilde{\omega}_{n_1} + \tilde{\omega}_{n_2} - \tilde{\omega}_{p_1} - \tilde{\omega}_{p_2})t''} \right\}. \tag{34}$$

Here, n_1 and n_2 are both assumed to sit far away from the pump modes in frequency and $n_1 \neq n_2$ is understood. Now that we have our analytic perturbative solutions for the evolution of one- and two-photon generation processes, we apply these to a simple system in the following sections.

To the best of our knowledge, the analytic expressions given in Eqs. (33) and (34) are new. They can be used to calculate the system photon operator expectations in the presence of scattering loss in a wide variety of coupled-cavity systems.

IV. LOSSY DYNAMICS OF PHOTON PAIR GENERATION

To demonstrate the impact of loss on the pair-generation process, we consider a simple coupled-cavity model in which there are only three QMs, one for each of the signal, idler, and pump photons. For example, these could be the resonant frequencies of the three coupled cavities in the so-called photonic molecule structures in photonic crystal slabs [57]. For simplicity, we also assume that the signal and idler frequencies are in resonance with the pump frequency such that $\omega_s + \omega_i = 2\omega_p$. This is a restriction imposed upon the real part of the frequencies only, as we wish to investigate the effect of QM loss on the pair-generation process under resonant conditions, where pair generation can be maximal. In addition, we assume that at $t = 0$, the pump photons are already loaded in the pump mode, perhaps using waveguide or fiber coupling. This loading process could be included in

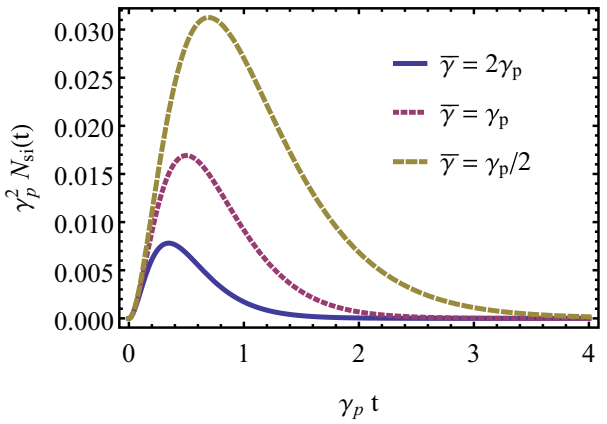

FIG. 2. (Color online) Dimensionless two-photon expectation in three cases: dashed (green) curve, when $\bar{\gamma} = \gamma_p/2$; dotted (red) curve, when $\bar{\gamma} = \gamma_p$; and solid (blue) curve, when $\bar{\gamma} = 2\gamma_p$.

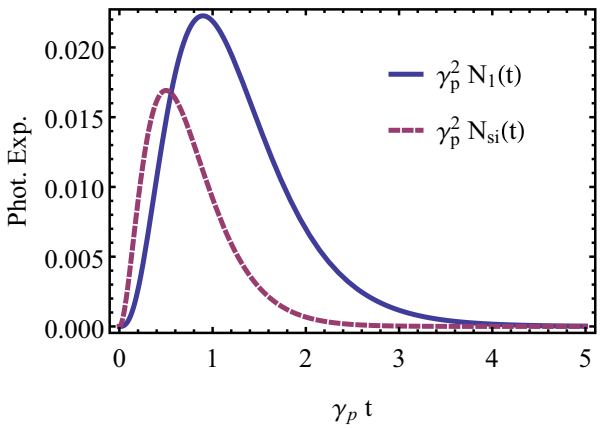

FIG. 3. (Color online) Comparison between the two-photon expectation and the only-one-photon expectation when $\bar{\gamma} = \gamma_p$. The two-photon expectation [dashed (red) curve] is compared to the only-one-photon expectation [solid (blue) curve]. Note that the plotted quantities are both dimensionless.

our model explicitly, but in this work we wish to focus on the physics of the generation process and so simply assume the initial state to be one with the pump mode in a coherent state in the pump mode. We will consider the more general situation in future work.

For this model, using Eq. (34), we define the scaled two-photon expectation to be

$$\begin{aligned} N_{si}(t) &\equiv \left\langle (b_s^\dagger b_s b_i^\dagger b_i)^{(2)}(t)\right\rangle / 8|G|^2 \\ &= e^{-4\gamma_p t}\int_0^t dt' e^{-2(\bar{\gamma}-\gamma_p)t'}\int_0^{t'} dt'' e^{-2(\bar{\gamma}-\gamma_p)t''} \\ &= \frac{e^{-4\bar{\gamma}t}(1-e^{-2(\bar{\gamma}-\gamma_p)t})^2}{8(\bar{\gamma}-\gamma_p)^2}. \end{aligned} \tag{35}$$

Here $G \equiv S_{m_s,m_i,p,p}|\alpha\phi_p|^2$ is simply a constant representing the coupling among the three modes in the presence of nonlinearity and $\bar{\gamma} = (\gamma_s + \gamma_i)/2$ is the average loss in the signal and idler modes. Note that this function depends only on the sum of the losses in the signal and idler modes, and not on each separately. As expected, at $t = 0$, there are no pairs, as this is our initial condition. The same is true when $t \to \infty$, since all of the photons have leaked out of the system. The two-photon expectation value (normalized to the effective nonlinear interaction strength) is shown as a function of time in Fig. 2. The results are plotted for three cases with different ratios of the average loss in the signal and idler, $\bar{\gamma}$, to the loss in the pump mode, γ_p. The general trend in all three cases is similar: there is a rise at early times due to the nonlinear generation followed by an exponential decay due to photon leakage. However, for a given pump loss, as $\bar{\gamma}$ increases the two-photon expectation value, in general, decreases.

Now let us consider the expectation value of the number of signal plus idler photons in the system that are not in pairs (due to the leakage out of the system of either a signal or an idler photon). This is given by the quantity

$$N_1(t) \equiv N_s(t) + N_i(t) - 2N_{si}(t), \tag{36}$$

where

$$\begin{aligned} N_s(t) &\equiv \left\langle (b_s^\dagger b_s)^{(2)}(t)\right\rangle / 8|G|^2 \\ &= e^{-4\gamma_p t}\int_0^t dt' e^{-2(\bar{\gamma}-\gamma_p)t'}\int_0^{t'} dt'' e^{-(\gamma_s-\gamma_i-2\gamma_p)t''} \\ &= \frac{e^{-4\gamma_p t}\left(\frac{1-e^{(4\gamma_p-2\gamma_s)t}}{4\gamma_p-2\gamma_s} + \frac{1-e^{-(2\bar{\gamma}-2\gamma_p)t}}{2\bar{\gamma}-2\gamma_p}\right)}{\gamma_s-\gamma_i-2\gamma_p} \end{aligned} \tag{37}$$

and

$$\begin{aligned} N_i(t) &\equiv \left\langle (b_i^\dagger b_i)^{(2)}(t)\right\rangle / 8|G|^2 \\ &= e^{-4\gamma_p t}\int_0^t dt' e^{-2(\bar{\gamma}-2\gamma_p)t'}\int_0^{t'} dt'' e^{-(\gamma_i-\gamma_s-2\gamma_p)t''} \\ &= \frac{e^{-4\gamma_p t}\left(\frac{1-e^{(4\gamma_p-2\gamma_i)t}}{4\gamma_p-2\gamma_i} + \frac{1-e^{-(2\bar{\gamma}-2\gamma_p)t}}{2\bar{\gamma}-2\gamma_p}\right)}{\gamma_i-\gamma_s-2\gamma_p}. \end{aligned} \tag{38}$$

Here signal and idler photons are counted separately, and the photons that are still in pairs are subtracted. Thus, this represents the one-photon-only expectation. Note that all the photon expectations presented here are related to internal photon generation and photon evolution in the system and do not represent the detection probabilities of these photons. We leave photon detection consideration for future work.

Depicted in Fig. 3 are the two-photon and one-photon-only expectations as a function of time, when $\bar{\gamma} = \gamma_p$. As shown, both paired and unpaired expectations have the same general behavior as a function of time. The rise time for the one-photon-only result is longer than that for the two-photon result. This occurs because the signal and idler photons must be generated first in order for them to decay into the one-photon state. Also, the one-photon-only curve has a larger maximum, so that at later times it is more likely for the system to be detected in a one-photon state when loss is present. At large times, the two-photon expectation decays approximately as $\exp(-4\gamma_p t)$, whereas the unpaired photons decay approximately as $\exp(-2\gamma_p t)$. Therefore, the one-photon-only state of the system decays more slowly, which

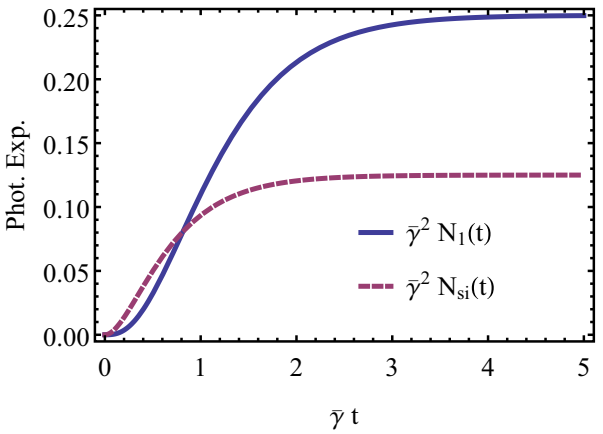

FIG. 4. (Color online) Photon dynamics when the pump mode is lossless but $\gamma_s = \gamma_i$. The two-photon expectation [dashed (red) curve] is compared to the one-photon-only expectation [solid (blue) curve]. Note that the plotted quantities are both dimensionless.

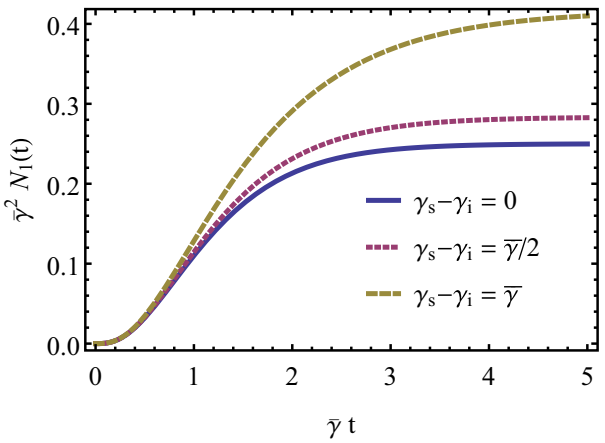

FIG. 5. (Color online) Dimensionless $N_1(t)$ as a function of time in three cases: solid (blue) curve, when $\gamma_s - \gamma_i = 0$; dotted (red) curve, when $\gamma_s - \gamma_i = \bar{\gamma}/2$; and dashed (green) curve, when $\gamma_s - \gamma_i = \bar{\gamma}$.

again confirms the higher probability of the system's carrying unpaired photons.

Note that if we assume that signal and idler modes are lossless, we can immediately conclude that $N_s(t) = N_i(t) = N_{si}(t)$, irrespective of the loss in the pump, so that $N_1(t) = 0$, in agreement with expectations. In this case, one never finds only one photon in the system, as the generated photon pairs do not leak out.

A. Lossless pump limit

Let us now consider the situation where the pump mode is lossless ($\gamma_p = 0$) but the signal and idler modes are not. In Fig. 4 we plot the photon-pair expectation along with the one-photon-only expectation when only the pump is lossless. We see that at long times, the expectation values tend to steady-state values given by

$$N_{si}(\infty) = 1/8\bar{\gamma}^2 \tag{39}$$

and

$$N_1(\infty) = 1/2\gamma_s\gamma_i - 1/4\bar{\gamma}^2. \tag{40}$$

In this case, because the pump photons last forever in the system, they can constantly convert into signal and idler photons, reaching a steady state at longer times. This would be the situation that would arise if we imagine that the photons in the pump mode are coupled in from outside at a rate such that the new photons added to the mode exactly balance those lost due to scattering losses. Since in the derivation of Eq. (33) and Eq. (34) no use of the undepleted pump approximation has been made, one might expect the photon expectation of the signal and idler modes to drop at long times. However, note that these results are at second order in perturbation theory and it can be shown that pump depletion does not appear to this order.

Note that the analytic expressions (39) and (40) suggest that one should keep the photon decay rates low if one wishes to obtain a high steady-state pair-generation rate. However, as we see later, there is a trade-off between the signal brightness and multiple pair generation that depends on the loss constants.

In Fig. 5, the one-photon-only expectation value is shown for different values of the difference between signal and idler photon loss rates, again, for the case where $\gamma_p = 0$. As shown, an increasing loss-rate difference results in higher values for the one-photon-only expectation, especially at longer times after generation. This means that any loss-rate difference between signal and idler photons increases the probability of a false signal heralding in the system.

V. EFFECT OF MULTIPLE PAIR GENERATION

As mentioned in Sec. I, one of the main challenges in obtaining a reliable heralded single-photon source is to keep the multiple pair generation as low as possible. We now discuss the lossy dynamics of multiple pairs using our Heisenberg approach. In the previous section, photon-number expectation values were examined. Here we examine the probability of finding multiple pairs as well as single pairs in the system. The probability of finding only one pair of signal and idler photons in the Heisenberg picture is

$$p_{11}(t) = \mathrm{Tr}(\rho_0 P_{11}(t)), \tag{41}$$

where ρ_0 is the initial state of the system given in Eq. (25) and $P_{11}(t)$ is the Heisenberg projection operator onto the $|1_s 1_i\rangle$ state corresponding to one photon in each one of the signal and idler modes. This projector is given by

$$P_{11}(t) = (b_s b_i)^\dagger(t)\,|\mathrm{vac}\rangle\,\langle\mathrm{vac}|\,(b_s b_i)(t). \tag{42}$$

Thus, the probability of finding a single pair in the system is

$$p_{11}(t) = |\langle\mathrm{vac}\,|(b_s b_i)(t)|\,\mathrm{vac}\rangle|^2. \tag{43}$$

In the same manner, the probability of finding two pairs due to second-order generation is

$$p_{22}(t) = |\langle\mathrm{vac}\,|(b_s b_s b_i b_i)(t)|\,\mathrm{vac}\rangle|^2. \tag{44}$$

We note that these quantities are distinct from detection probabilities, as they represent the probabilities of the photons being anywhere within the system, rather than at a particular position where there is a detector. Using our perturbative

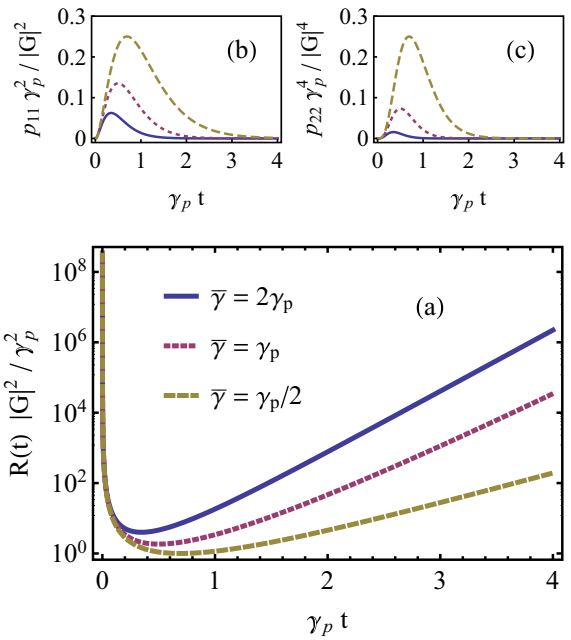

FIG. 6. (Color online) (a) Plot of the dimensionless noise figure $R(t)|G|^2/\gamma_p^2$ in three cases: dashed (green) curve, for $\bar{\gamma} = 2\gamma_p$; dotted (red) curve, for $\bar{\gamma} = \gamma_p$; and solid (blue) curve, for $\bar{\gamma} = \gamma_p/2$. (b, c) $p_{11}$and p_{22} as a function of time for the same conditions.

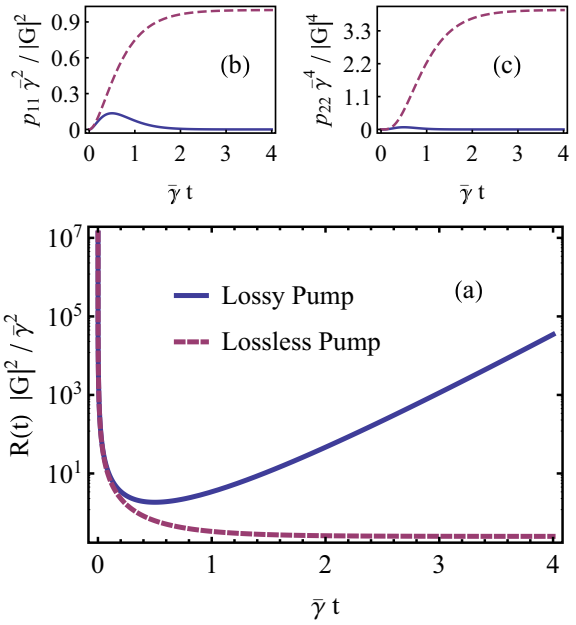

FIG. 7. (Color online) (a) Plot of the dimensionless $R(t)|G|^2/\bar{\gamma}^2$ in two cases: dashed (red) curve, when $\gamma_p = 0$; and solid (blue) curve, when $\bar{\gamma} = \gamma_p$. (b, c) $p_{11}$and p_{22} as a function of time for the same conditions.

treatment of the adjoint master equation and following procedures similar to those presented in the Appendixes, the first nonzero approximations (first order for p_{11} and second order for p_{22}) are found to be

$$p_{11}(t) = |G|^2 e^{-4\gamma_p t} \left(\frac{1 - e^{-2(\bar{\gamma}-\gamma_p)t}}{\bar{\gamma} - \gamma_p} \right)^2 \tag{45}$$

and

$$p_{22}(t) = 4\,|G|^4 e^{-8\gamma_p t} \left(\frac{1 - e^{-2(\bar{\gamma}-\gamma_p)t}}{\bar{\gamma} - \gamma_p} \right)^4 . \tag{46}$$

Note that the second-order contribution to $p_{11}(t)$ is in fact 0. These results are new and give compact, analytic expressions for the effect of scattering loss. Also, it can be observed that both these expressions depend only on the average loss in the signal and idler modes.

As a noise figure, we evaluate the ratio between the one-pair and two-pair probabilities,

$$R(t) \equiv p_{11}(t)/p_{22}(t). \tag{47}$$

Other noise contributors, such as dark counts, are not considered here. Thus, we see that R is proportional to the inverse of the pump intensity. This is analogous to what is observed in the experimental CAR at high powers and reflects the familiar trade-off between signal brightness and CAR in a typical experiment.

Figure 6 shows the noise figure R for different values of the average loss in the signal and idler modes. The probabilities p_{11} and p_{22} are shown separately as well. As shown, the noise figure is larger when the pump loss is smaller than the signal and idler average loss [solid (blue) curves]. This means that it is more likely that multiple pairs will be generated if the pump mode stays in the system longer.

In the case of a lossless pump, R reaches a steady-state value at longer times. This is illustrated in Fig. 7, which shows the noise figure for both a lossless and a lossy pump. For the lossless pump, R tends to the steady-state value

$$R(\infty) = \bar{\gamma}^2/4\,|G|^2\,, \tag{48}$$

as $t \to \infty$. As expected, this ratio scales as 1 over the pump field intensity. It is important to note that the steady-state value of R increases with increasing loss in the signal and idler modes. Therefore, although it is necessary to keep the signal and idler loss rates low if one wants a bright pair signal, there is a trade-off as lower losses result in higher rates of multiple pair generation. This is because the decay rate of multiple pairs is higher then that of a single pair. As shown, low loss rates for the signal and idler favor multiple pair generation in the steady state. The dimensionless quantity $|G|/\bar{\gamma}$ quantifies the trade-off between signal brightness and higher multiple pair-generation rates. This shows that in situations where the pump is constant in time, there is an optimum pump field amplitude that depends upon the loss in the signal and idler modes.

To be more precise, in the lossless pump regime the signal brightness steady-state value is directly proportional to the fundamental factor $|G|^2/\bar{\gamma}^2$, the exact same factor to which the noise figure R is inversely proportional. Therefore, from the device-design point of view, if one is interested in a certain noise figure R for a device, there is always a pump field amplitude that can achieve this, regardless of the loss rates in the system. At first glance it might seem to follow from this that loss can be simply neglected, with the only conequence being that for a smaller loss the source will be brighter at any given pump power. However, as shown in Fig. 6, it takes longer to obtain the same noise figure R for lower loss rates than for higher loss rates. This is unproblematic, as long as one is concerned only with avoiding multiple-pair generation.

But when loss is present it is also possible for idler photons to be detected even when signal photons are already lost, or vice versa, as discussed in Secs. I and IV. Using Eq. (39) and Eq. (40) it is easy to see that, in the lossless pump case at steady state, the ratio between unpaired photons and paired photons in the system is

$$\frac{N_1(\infty)}{N_{st}(\infty)} = \frac{4(\gamma_s + \Delta/2)}{\gamma_s} - 2, \tag{49}$$

where we have expressed everything in terms of the signal loss, γ_s, and the signal and idler loss difference, $\Delta = \gamma_s - \gamma_i$. For a fixed, nonzero value of Δ, this ratio starts at infinity when $\gamma_s \to 0$ and approaches the value of 2 when $\gamma_s \to \infty$. Thus, unless we are dealing with the ideal case where $\Delta = 0$, we can minimize false heralds and missed signal photons by designing a system with a high loss rate. Of course, the price to be paid is that a high loss rate results in a source with low brightness. To overcome this difficulty, it has been proposed [65] that a number of identical devices be multiplexed, and the optimization of this scenario has been studied theoretically [77,78]. Therefore, in practice one should design the individual photon pair sources to have a signal loss coefficient that is much larger than the difference between the signal and the idler loss coefficients; the multiplexing of the single-photon sources should then be designed to obtain the desired CAR and brightness.

VI. CONCLUSION

In this paper, the lossy photon dynamics of pair generation via SFWM has been treated in coupled-cavity systems. The QM basis of the coupled-cavity system, with complex frequencies, has been employed to include the intrinsic photon loss in the model. The full Hamiltonian was projected onto the QM basis to be used in the corresponding adjoint quantum master equation responsible for the time evolution of the different Heisenberg operators.

The linear part of the Hamiltonian results in a simple dynamics for any normal ordered chain of ladder operators. Using this simple result, the nonlinear Hamiltonian part was treated by means of perturbation to obtain approximate but analytic expressions for different Heisenberg operators of interest, such as those used in photon-number expectation and multiple pair-generation probabilities.

Lossy dynamics was studied in a simple three-mode system, with the frequencies for the pump, signal, and idler. For the three-mode model, it was shown that loss makes photon pairs decay into one-photon states, in particular, when unbalanced loss rates for signal and idler photons are considered. In addition, the effect of loss on multiple pair generation was studied. There is a trade-off between signal brightness and higher multiple pair generation that depends on the average loss rate of the signal and idler photons, which essentially derives from the faster decay of multiple pairs compared to single pairs.

Although in this work we have only applied our lossy Heisenberg approach to a three-mode system, the developed formalism is quite general and is capable of incorporating multiple modes in each one of the signal, idler, and pump bands. In fact, the derived expressions for the photon-number expectation in Sec. III carry sums corresponding to such situations.

We have applied our Heisenberg approach to treat pair generation via SFWM. However, generalization of the model to other nonlinear processes that might be of interest is possible. In addition to the coupled-cavity systems that are the focus of this work, any other system susceptible to a QM description might be treated this way. In particular, it is ideally suited to treat pair generation in CROWs and in ring resonators, both of which we leave for future work. In this paper, we have calculated photon numbers and the probability of finding photons anywhere within the structure. Our formalism can also be employed to determine the probability of photon detection for detectors placed, say, at the output port of a CROW or ring-resonator system. We plan to include the detection process in future work.

ACKNOWLEDGMENTS

This work was supported in part by the Natural Sciences and Engineering Research Council of Canada and by the Australian Research Council Centre of Excellence for Ultrahigh bandwidth Devices for Optical Systems (Project No. CE110001018).

APPENDIX A: SECOND-ORDER ANSATZ FOR THE NUMBER OPERATOR

In this Appendix, we present the main steps in deriving Eq. (33) for $\langle (b_n^\dagger b_n)^{(2)}(t)\rangle$. The second-order approximation to the photon-number expectation is governed by

$$\frac{d(b_n^\dagger b_n)^{(2)}(t)}{dt} = \mathcal{L}_0(b_n^\dagger b_n)^{(2)}(t) - \frac{i}{\hbar}[(b_n^\dagger b_n)^{(1)}(t), H_{\rm NL}] \tag{A1}$$

$$= \mathcal{L}_0(b_n^\dagger b_n)^{(2)}(t) + \left\{ i \sum_{m_2} \sum_{p_1,p_2} \sum_{m_1',m_2'} \sum_{p_1',p_2'} h^{(1)}_{n,m_2,p_1,p_2}(t) S_{m_1',m_2',p_1',p_2'} [b_n^\dagger b_{m_2}^\dagger b_{p_1} b_{p_2}, b_{m_1'}^\dagger b_{m_2'}^\dagger b_{p_1'} b_{p_2'}] + \text{H.c.} \right\}$$

$$+ \left\{ i \sum_{m_2} \sum_{p_1,p_2} \sum_{m_1',m_2'} \sum_{p_1',p_2'} h^{(1)}_{n,m_2,p_1,p_2}(t) S^*_{m_1',m_2',p_1',p_2'} [b_n^\dagger b_{m_2}^\dagger b_{p_1} b_{p_2}, b_{p_2'}^\dagger b_{p_1'}^\dagger b_{m_2'} b_{m_1'}] + \text{H.c.} \right\}. \tag{A2}$$

Consider the commutator on the second line of Eq. (A2), which involves only raising operators corresponding to signal and idler indices. Therefore, no matter what this commutator simplifies to, its expectation value in the initial state, (25), is 0. The

second commutator, on the other hand, simplifies to

$$\begin{aligned}
&\left[b_n^\dagger b_{m_2}^\dagger b_{p_1} b_{p_2}, b_{p_2'}^\dagger b_{p_1'}^\dagger b_{m_2'} b_{m_1'}\right] \\
&= b_n^\dagger b_{m_2}^\dagger b_{p_1'}^\dagger b_{p_1} b_{m_2'} b_{m_1'} \delta_{p_2 p_2'} + b_n^\dagger b_{m_2}^\dagger b_{p_2'}^\dagger b_{p_1} b_{m_2'} b_{m_1'} \delta_{p_2 p_1'} + b_n^\dagger b_{m_2}^\dagger b_{p_1'}^\dagger b_{p_2} b_{m_2'} b_{m_1'} \delta_{p_1 p_2'} + b_n^\dagger b_{m_2}^\dagger b_{p_2'}^\dagger b_{p_2} b_{m_2'} b_{m_1'} \delta_{p_1 p_1'} \\
&\quad + b_n^\dagger b_{m_2}^\dagger b_{m_2'} b_{m_1'} \delta_{p_2 p_2'} \delta_{p_1 p_1'} + b_n^\dagger b_{m_2}^\dagger b_{m_2'} b_{m_1'} \delta_{p_2 p_1'} \delta_{p_1 p_2'} - b_{p_2'}^\dagger b_{p_1'}^\dagger b_{m_2}^\dagger b_{m_2'} b_{p_1} b_{p_2} \delta_{m_1' n} - b_{p_2'}^\dagger b_{p_1'}^\dagger b_n^\dagger b_{m_2'} b_{p_1} b_{p_2} \delta_{m_1' m_2} \\
&\quad - b_{p_2'}^\dagger b_{p_1'}^\dagger b_{m_2}^\dagger b_{m_1'} b_{p_1} b_{p_2} \delta_{m_2' n} - b_{p_2'}^\dagger b_{p_1'}^\dagger b_n^\dagger b_{m_1'} b_{p_1} b_{p_2} \delta_{m_2' m_2} - b_{p_2'}^\dagger b_{p_1'}^\dagger b_{p_1} b_{p_2} \delta_{m_1' n} \delta_{m_2' m_2} - b_{p_2'}^\dagger b_{p_1'}^\dagger b_{p_1} b_{p_2} \delta_{m_1' m_2} \delta_{m_2' n}. \qquad \text{(A3)}
\end{aligned}$$

From all these, only the two terms that have four ladder operators and are negative in sign have a nonzero expectation value. Moreover, S_{m_1,m_2,p_1,p_2} and $h^{(1)}_{m_1,m_2,p_1,p_2}(t)$ in Eq. (A2) are invariant under index exchange $m_1 \leftrightarrow m_2$ ($p_1 \leftrightarrow p_2$). Therefore, we obtain

$$\left\langle \frac{d(b_n^\dagger b_n)^{(2)}(t)}{dt} \right\rangle = \langle \mathcal{L}_0 (b_n^\dagger b_n)^{(2)}(t) \rangle - \left\{ 2i \sum_{m_2} \sum_{p_1,p_2} \sum_{p_1',p_2'} h^{(1)}_{n,m_2,p_1,p_2}(t) S^*_{n,m_2,p_1',p_2'} \langle b_{p_2'}^\dagger b_{p_1'}^\dagger b_{p_1} b_{p_2} \rangle + \text{H.c.} \right\}. \qquad \text{(A4)}$$

As suggested by this equation, the second-order ansatz that we employ for the number operator corresponding to terms with only nonzero expectations is

$$(b_n^\dagger b_n)^{(2)}(t) = \sum_{p_1,p_2} \sum_{p_1',p_2'} h^{(2)}_{p_1,p_2,p_1',p_2'}(t)\, b_{p_2'}^\dagger b_{p_1'}^\dagger b_{p_1} b_{p_2} + \text{H.c.}. \qquad \text{(A5)}$$

Note that all other terms which we have not represented in our ansatz evolve independently from each other and from terms we have shown above, thus they will have no indirect contribution to the final expectation value. Substituting (A5) into (A1) and using simple dynamics of normally ordered operators under $\mathcal{L}_0$ presented in Eq. (10), we obtain the differential equation

$$\frac{dh^{(2)}_{p_1,p_2,p_1',p_2'}(t)}{dt} = i\left(\tilde{\omega}^*_{p_1'} + \tilde{\omega}^*_{p_2'} - \tilde{\omega}_{p_1} - \tilde{\omega}_{p_2}\right) h^{(2)}_{p_1,p_2,p_1',p_2'}(t) - 2i \sum_{m_1,m_2} h^{(1)}_{n,m_2,p_1,p_2}(t) S^*_{n,m_2,p_1',p_2'} \qquad \text{(A6)}$$

for $h^{(2)}_{p_1,p_2,p_1',p_2'}(t)$. Integrating this, we obtain

$$h^{(2)}_{p_1,p_2,p_1',p_2'}(t) = -2i \sum_{m_2} h^{(1)}_{n,m_2,p_1,p_2} S^*_{n,m_2,p_1',p_2'} e^{i(\tilde{\omega}^*_{p_1'} + \tilde{\omega}^*_{p_2'} - \tilde{\omega}_{p_1} - \tilde{\omega}_{p_2})t} \int_0^t dt' e^{-i(\tilde{\omega}^*_{p_1'} + \tilde{\omega}^*_{p_2'} - \tilde{\omega}_{p_1} - \tilde{\omega}_{p_2})t'}. \qquad \text{(A7)}$$

This can then be used to derive the photon-number expectation given by Eq. (33).

APPENDIX B: FIRST- AND SECOND-ORDER ANSATZEN FOR THE PRODUCT OF THE NUMBER OPERATORS

In this Appendix, we present the main steps in deriving Eq. (34) for $\langle (b_{n_1}^\dagger b_{n_1} b_{n_2}^\dagger b_{n_2})^{(2)}(t) \rangle$. For the product of the number operators, the zeroth-order evolution is simply

$$(b_{n_1}^\dagger b_{n_1} b_{n_2}^\dagger b_{n_2})^{(0)}(t) = e^{-2\gamma_{n_1} t} e^{-2\gamma_{n_2} t} b_{n_1}^\dagger b_{n_1} b_{n_2}^\dagger b_{n_2}. \qquad \text{(B1)}$$

This has zero expectation when operating on the vacuum, thus we continue with the first-order perturbation

$$\frac{d(b_{n_1}^\dagger b_{n_1} b_{n_2}^\dagger b_{n_2})^{(1)}(t)}{dt} = \mathcal{L}_0 \left(b_{n_1}^\dagger b_{n_1} b_{n_2}^\dagger b_{n_2}\right)^{(1)}(t) - \frac{i}{\hbar} \left[\left(b_{n_1}^\dagger b_{n_1} b_{n_2}^\dagger b_{n_2}\right)^{(0)}(t), H_{\text{NL}} \right]. \qquad \text{(B2)}$$

Unfortunately, this commutator does not yield as simple an expression as Eq. (28) for the first-order perturbation. However, it is easy to see that, if normally ordered, every term in this commutator has zero expectation value when operating on the vacuum for the signal and idler modes. On the other hand, some of the terms will eventually contribute to the expectation value for the product operator through the second-order perturbation. Only considering such terms, the proper ansatz for the first-order perturbation is

$$\left(b_{n_1}^\dagger b_{n_1} b_{n_2}^\dagger b_{n_2}\right)^{(1)}(t) = \sum_{p_1,p_2} g^{(1)}_{n_1,n_2,p_1,p_2}(t) b_{n_1}^\dagger b_{n_2}^\dagger b_{p_1} b_{p_2} + \text{H.c.}. \qquad \text{(B3)}$$

Substituting Eq. (B3) into Eq. (B2) gives a differential equation for the $g^{(1)}_{n_1,n_2,p_1,p_2}(t)$, which we integrate to obtain

$$g^{(1)}_{n_1,n_2,p_1,p_2}(t) = 2i S_{n_1,n_2,p_1,p_2} e^{i(\tilde{\omega}^*_{n_1} + \tilde{\omega}^*_{n_2} - \tilde{\omega}_{p_1} - \tilde{\omega}_{p_2})t} \int_0^t dt' e^{-2\gamma_{n_1} t'} e^{-2\gamma_{n_2} t'} e^{-i(\tilde{\omega}^*_{n_1} + \tilde{\omega}^*_{n_2} - \tilde{\omega}_{p_1} - \tilde{\omega}_{p_2})t'}. \qquad \text{(B4)}$$

This expression is then subjected to one final iteration of the dynamical master equation to derive the second-order evolution of the product of the number operators. It can be seen that the adjoint master equation for the expectation value of the product

operator is

$$\left\langle \frac{d(b^{\dagger}_{n_1} b_{n_1} b^{\dagger}_{n_2} b_{n_2})^{(2)}(t)}{dt} \right\rangle = \langle \mathcal{L}_0 (b^{\dagger}_{n_1} b_{n_1} b^{\dagger}_{n_2} b_{n_2})^{(2)}(t) \rangle - \left\{ 2i \sum_{p_1,p_2} \sum_{p_1',p_2'} h^{(1)}_{n_1,n_2,p_1,p_2}(t) S^{*}_{n_1,n_2,p_1',p_2'} \left\langle b^{\dagger}_{p_2'} b^{\dagger}_{p_1'} b_{p_1} b_{p_2} \right\rangle + \text{H.c.} \right\}. \tag{B5}$$

This means that the second-order ansatz for the product operator has to be set to

$$\left(b^{\dagger}_{n_1} b_{n_1} b^{\dagger}_{n_2} b_{n_2}\right)^{(2)}(t) = \sum_{p_1,p_2} \sum_{p_1',p_2'} g^{(2)}_{p_1,p_2,p_1',p_2'}(t) b^{\dagger}_{p_2'} b^{\dagger}_{p_1'} b_{p_1} b_{p_2} + \text{H.c.} \tag{B6}$$

The corresponding $g^{(2)}_{p_1,p_2,p_1',p_2'}(t)$ is

$$g^{(2)}_{p_1,p_2,p_1',p_2'}(t) = -2i g^{(1)}_{n_1,n_2,p_1,p_2}(t) S^{*}_{n_1,n_2,p_1',p_2'} e^{i(\tilde{\omega}^{*}_{p_1'} + \tilde{\omega}^{*}_{p_2'} - \tilde{\omega}_{p_1} - \tilde{\omega}_{p_2})t} \int_0^t dt' e^{-i(\tilde{\omega}^{*}_{p_1'} + \tilde{\omega}^{*}_{p_2'} - \tilde{\omega}_{p_1} - \tilde{\omega}_{p_2})t'}. \tag{B7}$$

The given $g^{(1)}_{n_1,n_2,p_1,p_2}(t)$ and $g^{(2)}_{p_1,p_2,p_1',p_2'}(t)$ found here may then be used to obtain the expectation value of the product of the number operators given by Eq. (34).

[1] S.-T. Ho, X. Zhang, and M. K. Udo, J. Opt. Soc. Am. B **12**, 1537 (1995).

[2] X. Li, J. Chen, P. Voss, J. Sharping, and P. Kumar, Opt. Express **12**, 3737 (2004).

[3] M. Ferrera, L. Razzari, D. Duchesne, R. Morandotti, Z. Yang, M. Liscidini, J. E. Sipe, S. Chu, B. E. Little, and D. J. Moss, Nat. Photon. **2**, 737 (2008).

[4] S. Clemmen, K. Phan Huy, W. Bogaerts, R. G. Baets, P. Emplit, and S. Massar, Opt. Express **17**, 16558 (2009).

[5] C. Xiong, C. Monat, A. S. Clark, C. Grillet, G. D. Marshall, M. J. Steel, J. Li, L. O. Faolain, T. F. Krauss, J. G. Rarity, and B. J. Eggleton, Opt. Lett. **36**, 3413 (2011).

[6] C. Xiong, G. D. Marshall, A. Peruzzo, M. Lobino, A. S. Clark, D.-Y. Choi, S. J. Madden, C. M. Natarajan, M. G. Tanner, R. H. Hadfield, S. N. Dorenbos, T. Zijlstra, V. Zwiller, M. G. Thompson, J. G. Rarity, M. J. Steel, B. Luther-Davies, B. J. Eggleton, and J. L. O'Brien, Appl. Phys. Lett. **98**, 051101 (2011).

[7] N. Matsuda, T. Kato, K.-i. Harada, H. Takesue, E. Kuramochi, H. Taniyama, and M. Notomi, Opt. Express **19**, 19861 (2011).

[8] H. Takesue, N. Matsuda, E. Kuramochi, and M. Notomi, Sci. Rep. **4**, 3913 (2014).

[9] J. Sharping, M. Fiorentino, and P. Kumar, Opt. Lett. **26**, 367 (2001).

[10] M. Fiorentino, P. Voss, J. Sharping, and P. Kumar, IEEE Photon. Tech. Lett. **14**, 983 (2002).

[11] J. Sharping, J. Chen, X. Li, and P. Kumar, Opt. Express **12**, 3086 (2004).

[12] X. Li, P. L. Voss, J. E. Sharping, and P. Kumar, Phys. Rev. Lett. **94**, 053601 (2005).

[13] H. Takesue and K. Inoue, Opt. Express **13**, 7832 (2005).

[14] S. Dyer, M. Stevens, B. Baek, and S. Nam, Opt. Express **16**, 9966 (2008).

[15] J. Rarity, J. Fulconis, J. Duligall, W. Wadsworth, and P. Russell, Opt. Express **13**, 534 (2005).

[16] J. Fulconis, O. Alibart, J. O'Brien, W. J. Wadsworth, and J. G. Rarity, Phys. Rev. Lett. **99**, 120501 (2007).

[17] J. Fulconis, O. Alibart, W. Wadsworth, and J. Rarity, New J. Phys. **9**, 276 (2007).

[18] A. McMillan, J. Fulconis, M. Halder, C. Xiong, J. Rarity, and W. Wadsworth, Opt. Express **17**, 6156 (2009).

[19] M. Halder, J. Fulconis, B. Cemlyn, A. Clark, C. Xiong, W. Wadsworth, and J. Rarity, Opt. Express **17**, 4670 (2009).

[20] A. Clark, B. Bell, J. Fulconis, M. Halder, B. Cemlyn, A. Olivier, C. Xiong, W. Wadsworth, and J. Rarity, New J. Phys. **13**, 065009 (2011).

[21] J. Fan, A. Dogariu, and L. Wang, Opt. Lett. **30**, 1530 (2005).

[22] J. Chen, K. Lee, C. Liang, and P. Kumar, Opt. Lett. **31**, 2798 (2006).

[23] J. Spring, P. Salter, B. Metcalf, P. Humphreys, M. Moore, N. Thomas-Peter, M. Barbieri, X.-M. Jin, N. Langford, W. Kolthammer, M. Booth, and I. Walmsley, Opt. Express **21**, 13522 (2013).

[24] M. Collins, A. Clark, J. He, D.-Y. Choi, R. Williams, A. Judge, S. Madden, M. Withford, M. Steel, B. Luther-Davies, C. Xiong, and B. Eggleton, Opt. Lett. **37**, 3393 (2012).

[25] J. He, C. Xiong, A. Clark, M. Collins, X. Gai, D.-Y. Choi, S. Madden, B. Luther-Davies, and B. Eggleton, J. Appl. Phys. **112**, 123101 (2012).

[26] J. Sharping, K. Lee, M. Foster, A. Turner, B. Schmidt, M. Lipson, A. Gaeta, and P. Kumar, Opt. Express **14**, 12388 (2006).

[27] K. Harada, H. Takesue, H. Fukuda, T. Tsuchizawa, T. Watanabe, K. Yamada, Y. Tokura, and S. Itabashi, Opt. Express **16**, 20368 (2008).

[28] K. Harada, H. Takesue, H. Fukuda, T. Tsuchizawa, T. Watanabe, K. Yamada, Y. Tokura, and S. Itabashi, New J. Phys. **13**, 065005 (2011).

[29] S. Clemmen, A. Perret, S. Selvaraja, W. Bogaerts, D. van Thourhout, R. Baets, P. Emplit, and S. Massar, Opt. Lett. **35**, 3483 (2010).

[30] S. Azzini, D. Grassani, M. Strain, M. Sorel, L. Helt, J. Sipe, M. Liscidini, M. Galli, and D. Bajoni, Opt. Express **20**, 23100 (2012).

[31] C. Xiong, C. Monat, M. Collins, L. Tranchant, D. Petiteau, A. Clark, C. Grillet, G. Marshall, M. Steel, J. Li, L. O'Faolain, T. Krauss, and B. Eggleton, IEEE J. Sel. Topics Quantum Electron. **18**, 1676 (2012).

[32] M. Davanço, J. R. Ong, A. B. Shehata, A. Tosi, I. Agha, S. Assefa, F. Xia, W. M. J. Green, S. Mookherjea, and K. Srinivasan, Appl. Phys. Lett. **100**, 261104 (2012).
[33] N. Matsuda, H. Takesue, K. Shimizu, Y. Tokura, E. Kuramochi, and M. Notomi, Opt. Express **21**, 8596 (2013).
[34] W. Jiang, X. Lu, J. Zhang, O. Painter, and Q. Lin, arXiv:1210.4455.
[35] A. S. Clark, C. Husko, M. J. Collins, G. Lehoucq, S. Xavier, A. De Rossi, S. Combrié, C. Xiong, and B. J. Eggleton, Opt. Lett. **38**, 649 (2013).
[36] A. Christ, A. Fedrizzi, H. Hübel, T. Jennewein, and C. Silberhorn, in *Single-Photon Generation and Detection—Physics and Applications*, edited by J. F. A. Migdall, S. Polyakov, and J. C. Bienfang (Academic Press, New York, 2013).
[37] P. G. Kwiat, K. Mattle, H. Weinfurter, A. Zeilinger, A. V. Sergienko, and Y. Shih, Phys. Rev. Lett. **75**, 4337 (1995).
[38] O. Alibart, D. Ostrowsky, P. Baldi, and S. Tanzilli, Opt. Lett. **30**, 1539 (2005).
[39] M. Fiorentino, S. Spillane, R. Beausoleil, T. Roberts, P. Battle, and M. Munro, Opt. Express **15**, 7479 (2007).
[40] R. Rangarajan, M. Goggin, and P. Kwiat, Opt. Express **17**, 18920 (2009).
[41] T. Zhong, F. Wong, T. Roberts, and P. Battle, Opt. Express **17**, 12019 (2009).
[42] M. Hunault, H. Takesue, O. Tadanaga, Y. Nishida, and M. Asobe, Opt. Lett. **35**, 1239 (2010).
[43] A. Martin, A. Issautier, H. Herrmann, W. Sohler, D. Ostrowsky, O. Alibart, and S. Tanzilli, New J. Phys. **12**, 103005 (2010).
[44] A. Halevy, E. Megidish, L. Dovrat, H. Eisenberg, P. Becker, and L. Bohatý, Opt. Express **19**, 20420 (2011).
[45] S. V. Zhukovsky, L. G. Helt, P. Abolghasem, D. Kang, J. E. Sipe, and A. S. Helmy, J. Opt. Soc. Am. B **29**, 2516 (2012).
[46] R. T. Horn, P. Kolenderski, D. Kang, P. Abolghasem, C. Scarcella, A. Della Frera, A. Tosi, L. G. Helt, S. V. Zhukovsky, J. E. Sipe, G. Weihs, A. S. Helmy, and T. Jennewein, Sci. Rep. **3**, 2314 (2013).
[47] A. Vallés, M. Hendrych, J. Svozilìk, R. Machulka, P. Abolghasem, D. Kang, B. J. Bijlani, A. S. Helmy, and J. P. Torres, Opt. Express **21**, 10841 (2013).
[48] Z. Yang and J. E. Sipe, Opt. Lett. **32**, 3296 (2007).
[49] Z. Yang, P. Chak, A. D. Bristow, H. M. van Driel, R. Iyer, J. S. Aitchison, A. L. Smirl, and J. E. Sipe, Opt. Lett. **32**, 826 (2007).
[50] S. Azzini, D. Grassani, M. Galli, L. C. Andreani, M. Sorel, M. J. Strain, L. G. Helt, J. E. Sipe, M. Liscidini, and D. Bajoni, Opt. Lett. **37**, 3807 (2012).
[51] E. Engin, D. Bonneau, C. M. Natarajan, A. S. Clark, M. G. Tanner, R. H. Hadfield, S. N. Dorenbos, V. Zwiller, K. Ohira, N. Suzuki, H. Yoshida, N. Iizuka, M. Ezaki, J. L. O'Brien, and M. G. Thompson, Opt. Express **21**, 27826 (2013).
[52] S. Ishii, K. Nozaki, and T. Baba, Jpn. J. Appl. Phys. **45**, 6108 (2006).
[53] S. J. Devitt, A. D. Greentree, R. Ionicioiu, J. L. O'Brien, W. J. Munro, and L. C.-L. Hollenberg, Phys. Rev. A **76**, 052312 (2007).
[54] A. R. A. Chalcraft, S. Lam, B. D. Jones, D. Szymanski, R. Oulton, A. C. T. Thijssen, M. S. Skolnick, D. M. Whittaker, T. F. Krauss, and A. M. Fox, Opt. Express **19**, 5670 (2011).
[55] N. Caselli, F. Intonti, F. Riboli, A. Vinattieri, D. Gerace, L. Balet, L. H. Li, M. Francardi, A. Gerardino, A. Fiore, and M. Gurioli, Phys. Rev. B **86**, 035133 (2012).
[56] M. Soljačić and J. D. Joannopoulos, Nat. Mater. **3**, 211 (2004).
[57] S. Azzini, D. Grassani, M. J. Strain, P. Velha, M. Sorel, L. G. Helt, J. E. Sipe, D. Gerace, M. Liscidini, M. Galli, and D. Bajoni, in *CLEO: 2013* (Optical Society of America, Washington, DC, 2013), p. QTh1E.3.
[58] H. Takesue and K. Shimizu, Opt. Commun. **283**, 276 (2010).
[59] A. R. Cowan and J. F. Young, Phys. Rev. E **68**, 046606 (2003).
[60] S. F. Mingaleev, A. E. Miroshnichenko, Y. S. Kivshar, and K. B. Busch, Phys. Rev. E **74**, 046603 (2006).
[61] Q. Lin, O. J. Painter, and G. P. Agrawal, Opt. Express **15**, 16604 (2007).
[62] J. Bravo-abad, S. Fan, S. G. Johnson, J. D. Joannopoulos, and M. Soljačić, J. Lightwave Technol. **25**, 2539 (2007).
[63] Z. Yang, M. Liscidini, and J. E. Sipe, Phys. Rev. A **77**, 033808 (2008).
[64] M. Liscidini, L. G. Helt, and J. E. Sipe, Phys. Rev. A **85**, 013833 (2012).
[65] M. J. Collins, C. Xiong, I. H. Rey, T. D. Vo, J. He, S. Shahnia, C. Reardon, T. F. Krauss, M. J. Steel, A. S. Clark, and B. J. Eggleton, Nat. Commun. **4**, 2582 (2013).
[66] L. J. Wang, C. K. Hong, and S. R. Friberg, J. Opt. B: Quantum Semiclass. **3**, 346 (2001).
[67] Q. Lin, F. Yaman, and G. P. Agrawal, Opt. Lett. **31**, 1286 (2006).
[68] Q. Lin and G. P. Agrawal, Opt. Lett. **31**, 3140 (2006).
[69] L. G. Helt, Z. Yang, M. Liscidini, and J. E. Sipe, Opt. Lett. **35**, 3006 (2010).
[70] H. Takesue, IEEE J. Select. Top. Quantum Electron. **18**, 1722 (2012).
[71] N. A. Silva and A. N. Pinto, IEEE J. Quantum Electron. **48**, 1380 (2012).
[72] D. P. Fussell and M. M. Dignam, Phys. Rev. A **77**, 053805 (2008).
[73] M. M. Dignam and M. Kamandar Dezfouli, Phys. Rev. A **85**, 013809 (2012).
[74] H.-P. Breuer and F. Petruccione, *The Theory of Open Quantum Systems* (Oxford University Press, New York, 2007).
[75] J. E. Sipe, J. Opt. A: Pure Appl. Opt. **11**, 114006 (2009).
[76] Although photon generation near the pump band can take place, it is unobservable in practice due to the need to filter the pump.
[77] I. S. P. Adam, M. Mechler, and M. Koniorczyk, arXiv:1408.3266 [quant-ph].
[78] R. J. Francis-Jones and P. J. Mosley, arXiv:1409.1394 [quant-ph].

Physical Review A (Atomic, Molecular and Optical Physics)

Title Details | Table of Contents

Basic Description

Title	Physical Review A (Atomic, Molecular and Optical Physics)
ISSN	1050-2947
Publisher	American Physical Society
Country	United States
Status	Active
Start Year	1893
Frequency	Monthly
Volume Ends	Jun - Dec
Language of Text	Text in: English
Refereed	Yes
Abstracted / Indexed	Yes
Serial Type	Journal
Content Type	Academic / Scholarly
Format	Print
Website	http://pra.aps.org
Email	pra@aps.org
Description	Contains articles on fundamental concepts of quantum mechanics, atomic and molecular structure and dynamics, collisions and interactions, molecular clusters, atomic and molecular processes in electromagnetic fields, and quantum optics.